arXiv:1603.08278v2 [cond-mat.soft] 23 May 2016

Phase Diagrams and Ordering in Charged Membranes: Binary Mixtures of Charged and Neutral Lipids

Naofumi Shimokawa*, Hiroki Himeno,† Tsutomu Hamada, and Masahiro Takagi
School of Materials Science, Japan Advanced Institute of Science and Technology, Ishikawa 923-1292, Japan

Shigeyuki Komura
Department of Chemistry, Graduate School of Science and Engineering, Tokyo Metropolitan University, Tokyo 192-0397, Japan

David Andelman
School of Physics and Astronomy, Raymond and Beverly Sackler Faculty of Exact Sciences, Tel Aviv University, Ramat Aviv 69978, Tel Aviv, Israel

(Dated: May 24, 2016)

We propose a model describing the phase behavior of two-component membranes consisting of binary mixtures of electrically charged and neutral lipids. We take into account the structural phase transition (main-transition) of the hydrocarbon chains, and investigate the interplay between this phase transition and the lateral phase separation. The presence of charged lipids significantly affects the phase behavior of the multicomponent membrane. Due to the conservation of lipid molecular volume, the main-transition temperature of charged lipids is lower than that of neutral ones. Furthermore, as compared with binary mixtures of neutral lipids, the membrane phase separation in binary mixtures of charged lipids is suppressed, in accord with recent experiments. We distinguish between two types of charged membranes: mixtures of charged saturated lipid/neutral unsaturated lipid and a second case of mixtures of neutral saturated lipid/charged unsaturated lipid. The corresponding phase behavior is calculated and shown to be very different. Finally, we discuss the effect of added salt on the phase separation and the temperature dependence of the lipid molecular area.

I. INTRODUCTION

Biomembranes are composed of various components such as phospholipids, sterols, and proteins, and are believed to have compositional heterogeneities. In multicomponent membranes, regions or domains enriched in saturated lipid and cholesterol are called "rafts", and are thought to play an important role in various biocellular functions, such as signal transduction and membrane trafficking [1, 2]. Artificial bilayer membranes composed of several phospholipids and cholesterol have been used as typical model systems for biomembranes. Phase separation in such model membranes has been widely investigated in order to understand the mechanism of raft formation [3]. Considerable effort has been given to ternary systems composed of saturated lipid, unsaturated lipid and cholesterol, where it is known that domains enriched in saturated lipid and cholesterol form a liquid-ordered phase in a matrix of an otherwise liquid-disordered phase [4–10].

Two-component lipid bilayers consisting of saturated and unsaturated lipids also show a phase separation between solid-like (L_β) and liquid-like (L_α) phases. This phase separation can be directly visualized by fluorescence microscopy, which demonstrates that the solid-like L_β domains exhibit various anisotropic shapes [11–14]. The resulting phase diagrams of different binary mixtures have been experimentally explored in great detail [14–18], and have been quantitatively reproduced in several theoretical works [19–23]. In particular, in models proposed by some of the present authors [19, 20, 22], a coupling between the membrane composition and its internal structure was suggested in order to consider the interplay between the phase separation and the chain phase transition (main-transition). In these experimental and theoretical studies, however, the lipids were taken to be electrically neutral.

Since a certain amount of charged lipid is always present in organelles such as mitochondria and lysosomes [24], electrostatic interactions are significant in biomembranes. Recently, several experiments have investigated the phase separation of multicomponent lipid mixtures containing at least one type of charged phospholipid [25–30]. In binary mixtures of neutral saturated lipid and negatively charged unsaturated lipid, the phase-separated region was suppressed as compared with the case when both lipids are neutral. This phase-separated region reappears when salt (e.g., NaCl), which screens the electrostatic interactions, was added. This is a strong indication that the electrostatic interaction affects the phase behavior. Although such behavior has been qualitatively explained by phenomenological models using the Poisson-Boltzmann (PB) theory [26, 31, 32], the structural phase transition (the main-transition) of the membrane was not considered.

*nshimo@jaist.ac.jp
†Also at Health Research Institute, National Institute of Advanced Industrial Science and Technology (AIST), Kagawa 761-0395, Japan

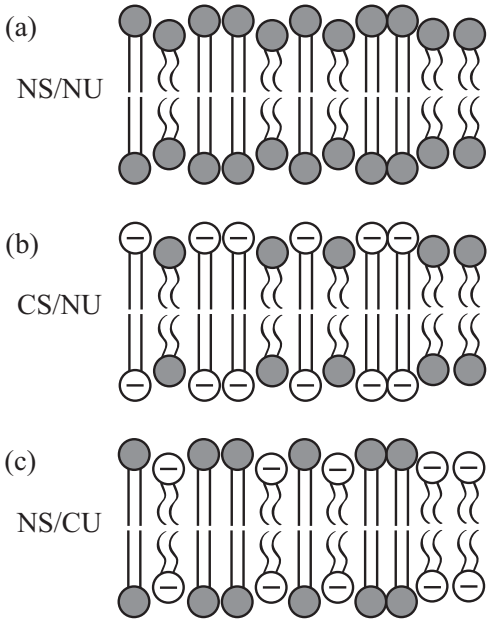

FIG. 1: Schematic illustration of two-component membranes. (a) A neutral membrane consisting of a binary mixture of neutral saturated (NS) and neutral unsaturated (NU) lipids. (b) A charged membrane consisting of a binary mixture of charged saturated (CS) and neutral unsaturated (NU) lipids. (c) A charged membrane consisting of a binary mixture of neutral saturated (NS) and charged unsaturated (CU) lipids.

In membranes composed of binary mixtures of neutral and charged lipids, either the saturated or unsaturated lipids can be charged. Hence, it is convenient to define two types of charged membranes: (i) mixtures of charged saturated (CS) and neutral unsaturated (NU) lipids (denoted as CS/NU, see Fig. 1(b)), and (ii) mixtures of neutral saturated (NS) and charged unsaturated (CU) lipids (denoted as NS/CU, see Fig. 1(c)). In recent experiments by Himeno *et al.* [29], it was reported that the phase separation was suppressed in the NS/CU lipid mixture as compared with the neutral membrane (NS/NU as in Fig. 1(a)), while it was enhanced in the CS/NU case. This result indicates that the phase behavior of charged membranes is very different between these two types of charged mixtures.

Being motivated by this experimental work, we consider in this paper charged membranes, and propose a phenomenological model that distinguishes between the above-mentioned two cases. In particular, we discuss the interplay between the main-transition and the lateral phase separation between the two lipid species. The main-transition of lipid chains is taken into account by extending the model of Goldstein and Leibler [33, 34] to include electrostatic interactions using the PB theory [35, 36]. Furthermore, we employ the constraint of constant molecular volume of the lipids, which leads to a coupling between the electrostatic interactions and the lipid lateral phase separation. We calculate the different phase diagrams of charged membranes by changing the interaction between the two lipids and/or by changing the amount of added salt. We also explain the different combination of hydrocarbon saturation and headgroup charge (either CS/NU or NS/CU as were defined above). On the basis of the calculated phase diagrams, we discuss the main-transition temperature, and the effect of added salt in a binary mixture of charged/neutral lipids.

In the next section, we explain the model by Goldstein and Leibler, the phase separation, and the PB theory. In Sec. III, we show the calculated phase diagrams and investigate the effects of the interaction between the two lipids, salt concentration, and combination of the lipids (either CS/NU or NS/CU) on the phase separation. Moreover, we explore how the molecular area changes and its dependence on the added salt. Finally, we offer a qualitative discussion in Sec. IV and some concluding remarks in Sec. V.

II. MODEL

In order to calculate the phase diagrams of binary mixtures of charged lipid membranes, we consider a model that takes into account both the lipid main-transition and the lateral lipid phase separation. For simplicity, we consider a perfectly flat membrane ignoring any possible out-of-plane membrane undulations. To avoid further complexity, we do not consider any specific bilayer attributes such as asymmetric lipid composition between the two leaflets, or ionic strength difference between the electrolytes in contact with the two sides of the membrane. Therefore, our model describes the phase behavior of an isolated symmetric bilayer.

A. Two-Component Neutral Membranes

On the basis of the Goldstein-Leibler model [33, 34], we first review the free energy of a single-component neutral lipid membrane, which leads to the main-transition. The main-transition involving the chain ordering and stiffening is described via a scalar order parameter

$$m = \frac{\delta - \delta_0}{\delta_0}, \tag{1}$$

where δ is the actual membrane thickness and δ_0 a reference membrane thickness in the L_α phase. Notice that m represents the changes that may occur in several degrees of freedom, including the conformation of the hydrocarbon chains, their interchain correlations, molecular tilt, and positional ordering. For an isolated lipid bilayer, a Landau expansion of the stretching freeenergy per lipid molecule in powers of the order parameter m is given by

$$f_{\rm st}(m) = \frac{a_2'}{2}(T - T^*)m^2 + \frac{a_3}{3}m^3 + \frac{a_4}{4}m^4, \tag{2}$$

where $a_2' > 0$, $a_3 < 0$, and $a_4 > 0$ are phenomenological coefficients. Here a_3 is taken to be negative since the main-transition is a first-order transition [16], while a_4 is always positive to ensure thermodynamical stability. In the above, T is the temperature and T^* is a reference temperature. The main-transition temperature is different from T^* and is denoted by T^{**}. It can be calculated from the conditions $f_{\rm st} = 0$ and $\mathrm{d}f_{\rm st}/\mathrm{d}m = 0$, yielding

$$T^{**} = T^* + \frac{2(a_3)^2}{9a_2'a_4}. \tag{3}$$

Note that the main-transition temperature described by Eq. (3) is appropriate only for neutral lipids.

Next, we describe the phase separation in membranes containing a binary mixture of neutral saturated (NS) and neutral unsaturated (NU) lipids, as shown in Fig. 1(a). We model the two-component membrane as an incompressible NS/NU lipid mixture containing ϕ molar fraction of NS lipid and $1-\phi$ molar fraction of NU lipid. (Throughout this paper, ϕ denotes the molar fraction of saturated lipid.) For simplicity, we assume the same area per molecule for the two species in the L_α phase and ignore any lipid exchange with the surrounding solvent. The mixing free energy (per lipid molecule) consists of the mixing entropy and enthalpy. It can be expressed within mean-field theory as

$$f_{\rm mix}(\phi) = k_{\rm B}T[\phi\ln\phi + (1-\phi)\ln(1-\phi)] + \frac{J}{2}\phi(1-\phi), \tag{4}$$

where $k_{\rm B}$ is the Boltzmann constant and $J > 0$ is an attractive interaction parameter between the lipids, which enhances the NS/NU demixing.

In general, the two lipids have different main-transition temperatures originating from different molecular parameters such as their chain length, degree of saturation and hydrophilic headgroup. The dependence of the main-transition temperature on the composition ϕ, cannot be calculated from such a phenomenological approach. Therefore, we proceed by further assuming the simplest linear interpolation of T^* as a function of ϕ:

$$T^*(\phi) = \phi T_{\rm S}^* + (1-\phi)T_{\rm U}^*, \tag{5}$$

where $T_{\rm S}^*$ and $T_{\rm U}^*$ are the reference temperatures of pure NS and NU lipids, respectively. In general, saturated lipids have higher transition temperatures than the unsaturated ones, $T_{\rm S}^{**} > T_{\rm U}^{**}$, for the cases when the numbers of hydrocarbons in the lipid tails are the same. Therefore we generally use $T_{\rm S}^* > T_{\rm U}^*$.

By combining Eqs. (2) and (4), we obtain the total free energy of a neutral NS/NU membrane

$$f_{\rm NS/NU}(m,\phi) = f_{\rm st}(m,\phi) + f_{\rm mix}(\phi). \tag{6}$$

This total free energy will be minimized with respect to both m and ϕ to obtain the phase behavior of a neutral membrane.

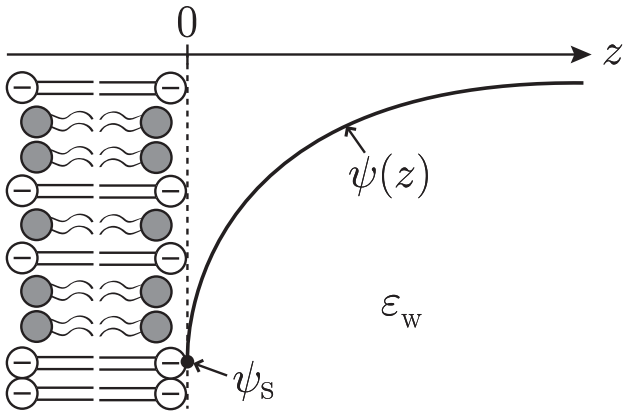

FIG. 2: Schematic representation of the electrostatic potential of a two-component charged membrane consisting of charged saturated (CS) and neutral unsaturated (NU) lipids. The lipid head groups are located at the plane $z = 0$. The dimensionless electrostatic potential in solution is $\psi(z) = e\Psi/k_{\rm B}T$, and $\psi_{\rm s} = \psi(z=0)$ is the surface potential at the membrane. The dielectric constant of water solution is $\varepsilon_{\rm w}$.

B. Electrostatic Free Energy of a Charged Membrane

In what follows, we extend the above model for the case of membranes consisting of a binary mixture of charged and neutral lipids. In order to estimate the electrostatic interactions in membranes at a fixed surface charge density (chosen to be negative throughout this paper), $\sigma < 0$, we obtain the free energy of a charged membrane on the basis of the PB theory [35, 36].

As shown in Fig. 2, we consider a flat charged lipid bilayer that lies at $z = 0$. The bilayer is in contact with a monovalent salt solution located at $z > 0$. We assume that the two leaflets constituting the bilayer do not interact with each other. Within a mean-field treatment, the electric potential $\Psi(z)$ satisfies the PB equation

$$\frac{\mathrm{d}^2\Psi}{\mathrm{d}z^2} = \frac{2en_{\rm b}}{\varepsilon_{\rm w}}\sinh\frac{e\Psi}{k_{\rm B}T}, \tag{7}$$

where e is the elementary charge, $n_{\rm b}$ the salt concentration in the bulk, and $\varepsilon_{\rm w}$ the dielectric constant of water. Using the dimensionless electric potential $\psi = e\Psi/k_{\rm B}T$, we obtain the following dimensionless PB equation

$$\frac{\mathrm{d}^2\psi}{\mathrm{d}z^2} = \kappa^2\sinh\psi, \tag{8}$$

where $\kappa^{-1} = \sqrt{\varepsilon_{\rm w}k_{\rm B}T/2e^2n_{\rm b}}$ is the Debye screening length. Far from the membrane, the bulk electric potential should vanish, i.e., $\psi(z\to\infty) = 0$. With the use of the Gauss law, the boundary condition at the membrane ($z = 0$) is

$$\varepsilon_{\rm w}\frac{\mathrm{d}\psi}{\mathrm{d}z}\bigg|_{z=0} = -\frac{e\sigma}{k_{\rm B}T}. \tag{9}$$

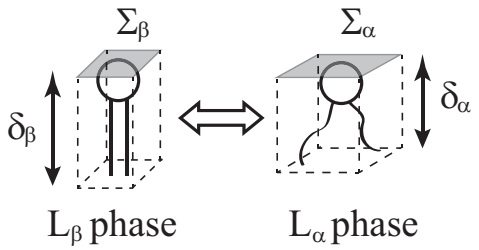

FIG. 3: Schematic illustration of molecular volume conservation. The molecular area is indicated by a gray square, and the molecular volume is enclosed by the dashed lines. We assume that the molecular volume v is conserved, $v = \Sigma_\beta\delta_\beta = \Sigma_\alpha\delta_\alpha$, for all the temperatures. The larger the membrane thickness δ, the smaller the molecular area Σ.

Under these boundary conditions, the dimensionless electric potential $\psi(z)$ can be obtained [35–37] by integrating twice Eq. (8)

$$\psi(z) = 2\ln\frac{1+\Gamma\exp(-\kappa z)}{1-\Gamma\exp(-\kappa z)}, \tag{10}$$

where

$$\Gamma = \frac{\exp(\psi_{\rm s}/2)-1}{\exp(\psi_{\rm s}/2)+1}. \tag{11}$$

Here $\psi_{\rm s} = \psi(z=0)$ is the dimensionless surface potential given by

$$\psi_{\rm s} = 2\sinh^{-1}\left(\frac{2\pi\ell_{\rm B}\sigma}{e\kappa}\right) = -2\sinh^{-1}\left(\frac{1}{b\kappa}\right), \tag{12}$$

where $\ell_{\rm B} = e^2/4\pi\varepsilon_{\rm w}k_{\rm B}T$ is the Bjerrum length, and $b = e/2\pi\ell_{\rm B}|\sigma|$ is the Gouy-Chapman length.

The electrostatic free energy per lipid molecule can be calculated from the charging method [37, 38]

$$f_{\rm el}(\sigma) = \frac{k_{\rm B}T\Sigma}{e}\int_0^\sigma {\rm d}\sigma'\,\psi_{\rm s}(\sigma'), \tag{13}$$

where Σ is the cross-sectional area per lipid. By substituting the surface potential, Eq. (12), into Eq. (13), we obtain the expression

$$f_{\rm el}(\sigma) = \frac{k_{\rm B}T\Sigma}{\pi\ell_{\rm B}b}\left[b\kappa - \sqrt{1+(b\kappa)^2} + \ln\frac{1+\sqrt{1+(b\kappa)^2}}{b\kappa}\right]. \tag{14}$$

C. Two-Component Charged Membranes

In the case of membranes consisting of a binary mixture of charged saturated (CS) and neutral unsaturated (NU) lipids, the surface charge density, $\sigma < 0$, is related to the CS molar fraction, ϕ, by

$$\sigma = -\frac{e\phi}{\Sigma}. \tag{15}$$

As illustrated in Fig. 3, we further assume that the lipid molecular volume, $v = \Sigma\delta$, is conserved and stays constant at any temperature. From Eq. (1), the cross-sectional area Σ is related to the order parameter, m, by

$$\Sigma = \frac{\Sigma_0}{1+m}, \tag{16}$$

where Σ_0 is the cross-sectional area of a neutral lipid in the L_α phase. By substituting back Eqs. (15) and (16) into Eq. (14), $f_{\rm el}$ can be written as

$$f_{\rm el}(m,\phi) = 2k_{\rm B}T\phi\left[\frac{1-\sqrt{1+[p\phi(1+m)]^2}}{p\phi(1+m)} + \ln\left(p\phi(1+m)+\sqrt{1+[p\phi(1+m)]^2}\right)\right], \tag{17}$$

where $p = 2\pi\ell_{\rm B}/\Sigma_0\kappa$ is a dimensionless parameter.

The total free energy of the CS/NU membrane is finally given by

$$f_{\rm CS/NU}(m,\phi) = f_{\rm st}(m,\phi) + f_{\rm mix}(\phi) + f_{\rm el}(m,\phi). \tag{18}$$

On the other hand, when the membrane consists of neutral saturated (NS) and charged unsaturated (CU) lipids, the total free energy of an NS/CU membrane becomes

$$f_{\rm NS/CU}(m,\phi) = f_{\rm st}(m,\phi) + f_{\rm mix}(\phi) + f_{\rm el}(m,1-\phi). \tag{19}$$

Note that the only change between the two cases, Eqs. (18) and (19), is that $\phi \leftrightarrow 1-\phi$ in the electrostatic free energy. The phase behavior of two-component charged membranes in these two cases is analyzed using either Eq. (18) or (19).

D. Equilibrium Phase Behavior

Since the electrostatic free energy described by Eq. (17) depends on the order parameter m, the main-transition temperature of a pure charged lipid (either CS or CU) is different from Eq. (3). Instead, it is given by the following conditions

$$f_{\rm st}(m_\beta,1) + f_{\rm el}(m_\beta,1) = f_{\rm st}(m_\alpha,1) + f_{\rm el}(m_\alpha,1), \tag{20}$$

$$\left.\frac{\partial(f_{\rm st}+f_{\rm el})}{\partial m}\right|_{m=m_\beta} = \left.\frac{\partial(f_{\rm st}+f_{\rm el})}{\partial m}\right|_{m=m_\alpha} = 0. \tag{21}$$

For lipid mixtures, the chemical potential μ is given by

$$\mu = \left.\frac{\partial f_{\rm tot}}{\partial\phi}\right|_{m=m^*}, \tag{22}$$

where $f_{\rm tot}$ is taken either from Eq. (6) for neutral membranes or Eqs. (18)–(19) for the two cases of charged membranes. The optimal order parameter, m^*, is obtained by minimizing the total free energy with respect to m, $\partial f_{\rm tot}/\partial m|_{m=m^*} = 0$.

TABLE I: Parameter Values of the Model

parameter	value	unit
a_2'	2.4×10^{-21}	J/K [34]
a_3	-1.1×10^{-18}	J [34]
a_4	2.2×10^{-18}	J [34]
$T_{\rm S}^*$	-10	°C
$T_{\rm U}^*$	-71	°C
Σ_0	65	Å^2
$\varepsilon_{\rm w}$	7.08×10^{-10}	F/m

As the lipid molar fraction ϕ is a conserved quantity, it is convenient to introduce another thermodynamic potential given by

$$g(\phi) = f_{\rm tot}(m = m^*, \phi) - \mu\phi. \tag{23}$$

The two-phase coexistence region in the (T, ϕ) plane is calculated by using the common tangent construction to account for the constraint value of the molar fraction ϕ. In other words, the two-phase coexistence has to satisfy the conditions $g(\phi_1) = g(\phi_2)$ and $\mu(\phi_1) = \mu(\phi_2)$, where the slope of the common tangent is equal to the chemical potential. From the coexisting two points in the (T, ϕ) plane, we can also construct the phase diagram in the (T, μ) plane. The $\rm L_\beta$ phase is characterized by positive m values, while its value in the $\rm L_\alpha$ phase becomes negative.

III. RESULTS

Having described our model in the previous section, we present the resulting phase diagrams and the temperature dependence of the molecular area. First, we show the phase diagrams for the neutral membrane case. This calculation essentially reproduces the theoretical results of Refs. [19, 20]. Then, the phase diagrams for charged membranes will be presented.

A. Choice of System Parameters

As examples for typical neutral saturated (NS) lipids and neutral unsaturated (NU) lipids, we consider, respectively, dipalmitoylphosphocholine (DPPC) and dioleoylphosphocholine (DOPC), whose main-transition temperature is $T_{\rm S}^{**} = 41\,^\circ$C and $T_{\rm U}^{**} = -20\,^\circ$C, respectively. From Eq. (3), the reference temperature of NS and NU lipids is set as $T_{\rm S}^* = -10\,^\circ$C and $T_{\rm U}^* = -71\,^\circ$C, respectively. The molecular area of the neutral lipid in the $\rm L_\alpha$ phase is fixed to $\Sigma_0 = 65\,$Å^2. The interaction parameter is $J = 1.2 \times 10^{-20}$ or $1.8 \times 10^{-20}\,$J as considered before [19, 20, 22], and the bulk salt concentration is chosen either as $n_{\rm b} = 1\,$M or $10\,$mM. All the parameters and physical constants used in our calculations are summarized in Table I.

B. Two-Component Neutral Membranes

For the NS/NU membrane, the total free energy is given in Eq. (6). As mentioned before, the NS lipid (whose molar fraction is ϕ) has a higher main-transition temperature than that of the NU lipid. Following Refs. [19, 20], we reproduce in Figs. 4 and 5 the phase diagrams of two-component NS/NU neutral membranes in the (T, ϕ) and the (T, μ) planes, respectively. Figures. 4(a) and 5(a) are calculated for $J = 1.2 \times 10^{-20}\,$J, while Figs. 4(b) and 5(b) are obtained for $J = 1.8 \times 10^{-20}\,$J. The main-transition temperature of NS ($\phi = 1$) and NU ($\phi = 0$) lipids is $T_{\rm S}^{**} = 41\,^\circ$C and $T_{\rm U}^{**} = -20\,^\circ$C, respectively. As shown in Fig. 4(a), we obtain three two-phase coexistence regions denoted by $\rm L_\alpha$+$\rm L_\beta^{(1)}$, $\rm L_\alpha$+$\rm L_\beta^{(2)}$, and $\rm L_\beta^{(1)}$+$\rm L_\beta^{(2)}$, and in Fig. 4(b), there are five two-phase coexistence regions indicated by $\rm L_\alpha^{(1)}$+$\rm L_\alpha^{(2)}$, $\rm L_\alpha^{(1)}$+$\rm L_\beta^{(1)}$, $\rm L_\alpha^{(1)}$+$\rm L_\beta^{(2)}$, $\rm L_\alpha^{(2)}$+$\rm L_\beta^{(2)}$, and $\rm L_\beta^{(1)}$+$\rm L_\beta^{(2)}$. As discussed before [19, 20], the phase-separated region is more extended when the interaction parameter J is larger.

C. Two-Component Charged Membranes

Next, we calculate the phase diagrams for two-component charged membranes. We first consider the charged saturated/neutral unsaturated (CS/NU) (Fig. 1(b)) lipid mixtures whose total free energy is given by Eq. (18). In Figs. 6(a) and 7(a), we show the calculated phase diagrams for $J = 1.2 \times 10^{-20}\,$J and $n_{\rm b} = 1\,$M, recalling that ϕ is the molar fraction of the CS lipids. The main-transition temperature of the CS lipid is calculated numerically from Eqs. (20) and (21) yielding $T_{\rm S}^{**} \simeq 29\,^\circ$C. On the other hand, the main-transition temperature of the NU lipid is $T_{\rm U}^{**} = -20\,^\circ$C, as before. In this phase diagram, there is only one coexistence region between the $\rm L_\alpha$ and $\rm L_\beta$ phases.

In Figs. 6(b) and 7(b), we obtain the phase diagrams for $J = 1.8 \times 10^{-20}\,$J, while the other parameters are the same as those in Figs. 6(a) and 7(a). The main-transition temperatures of the two lipids are unchanged, because the conditions in Eqs. (20) and (21) are independent of the interaction parameter J. In this case, there are three two-phase coexistence regions denoted by $\rm L_\alpha$+$\rm L_\beta^{(1)}$, $\rm L_\alpha$+$\rm L_\beta^{(2)}$, and $\rm L_\beta^{(1)}$+$\rm L_\beta^{(2)}$.

In order to further explore the effect of electrostatic interaction in CS/NU mixtures, we looked at the case of lower salinity. Figures 6(c) and 7(c) are the phase diagrams corresponding to the low salt case of $n_{\rm b} = 10\,$mM. The other parameters are the same as those in Figs. 6(a) and 7(a). The main-transition temperature of the CS lipid is now $T_{\rm S}^{**} \simeq 23\,^\circ$C, while that of the NU lipid is unchanged ($T_{\rm U}^{**} = -20\,^\circ$C). In this case, there is only one two-phase coexistence region between the $\rm L_\alpha$ and $\rm L_\beta$ phases.

Finally, we show in Figs. 6(d) and 7(d) the phase di-

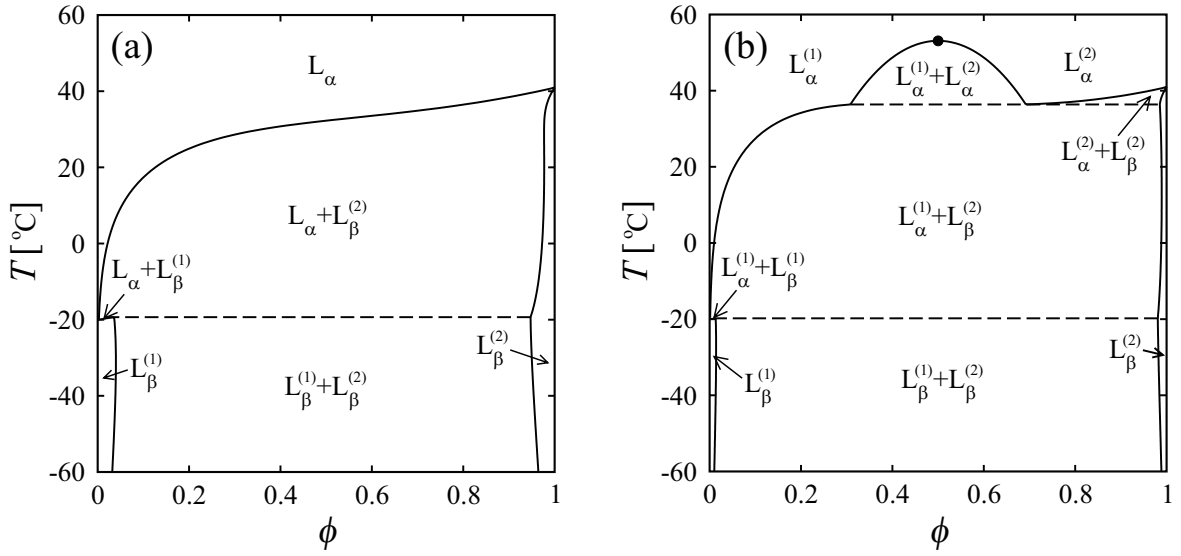

FIG. 4: Phase diagrams of a neutral NS/NU membrane as a function of the molar fraction, ϕ, of the NS lipids, and temperature T, reproducing the theoretical results of Refs. [19, 20]. The attractive interaction parameter J is chosen to be 1.2×10^{-20} J in part a and 1.8×10^{-20} J in part b. The other parameters are listed in Table I and are mentioned in the text. The critical point located at (ϕ_c, T_c)=(0.5, 53 °C) in part b is indicated by a filled circle. The horizontal dashed lines at $T = -19.2$ °C in part a, and $T = -19.7$ °C and $T = 36.4$ °C in part b indicate a three-phase coexistence (triple point).

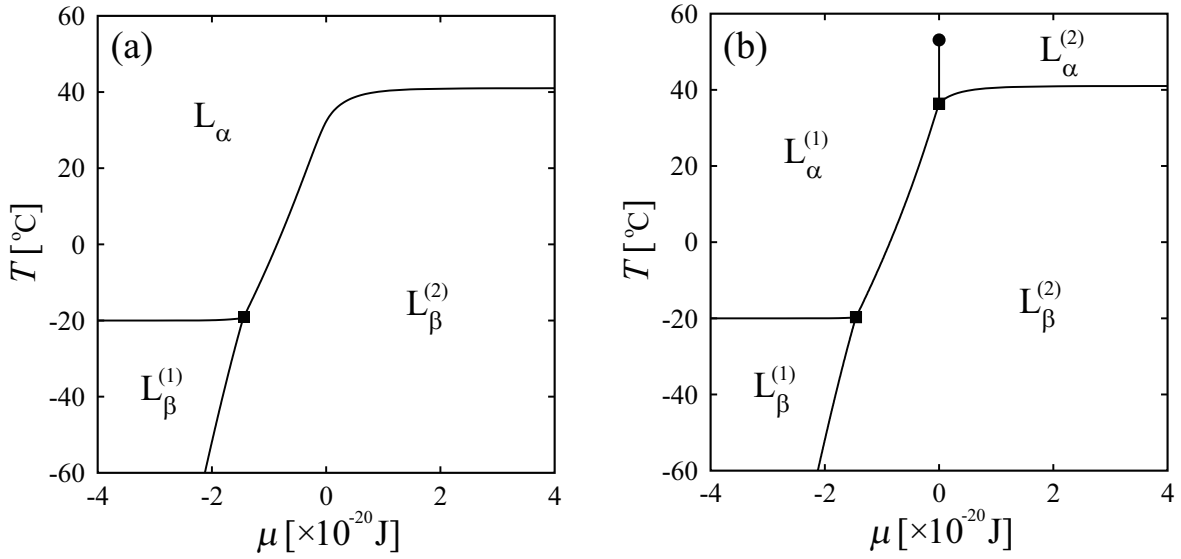

FIG. 5: Phase diagrams of a neutral NS/NU membrane as a function of the chemical potential, μ, of the NS lipids and temperature T. The attractive interaction parameter J is chosen to be 1.2×10^{-20} J in part a and 1.8×10^{-20} J in part b. The other parameters are listed in Table I and mentioned in the text. The critical point located at (μ_c, T_c)=(0 J, 53 °C) in part b is indicated by a filled circle. The filled squares located at (μ, T)=(-1.44×10^{-20} J, -19.2 °C) in part a, and (-1.45×10^{-20} J, -19.7 °C) and (0 J, 36.4 °C) in part b indicate the triple points.

agrams for the neutral saturated/charged unsaturated (NS/CU) lipid mixtures whose total free energy is given by Eq. (19). Notice that the molar fraction ϕ refers here to that of the NS lipids. The other parameters, J and n_b, are the same as those in Figs. 6(a) and 7(a). The main-transition temperature of the NS lipid is $T_S^{**} = 41$ °C, and that of the CU lipid is decreased to $T_U^{**} \simeq -30$ °C. There are three two-phase coexistence regions denoted by L_α+$L_\beta^{(1)}$, L_α+$L_\beta^{(2)}$, and $L_\beta^{(1)}$+$L_\beta^{(2)}$.

The phase behavior of two-component membranes depends on various quantities such as the interaction parameter J, the salt concentration n_b, and whether the

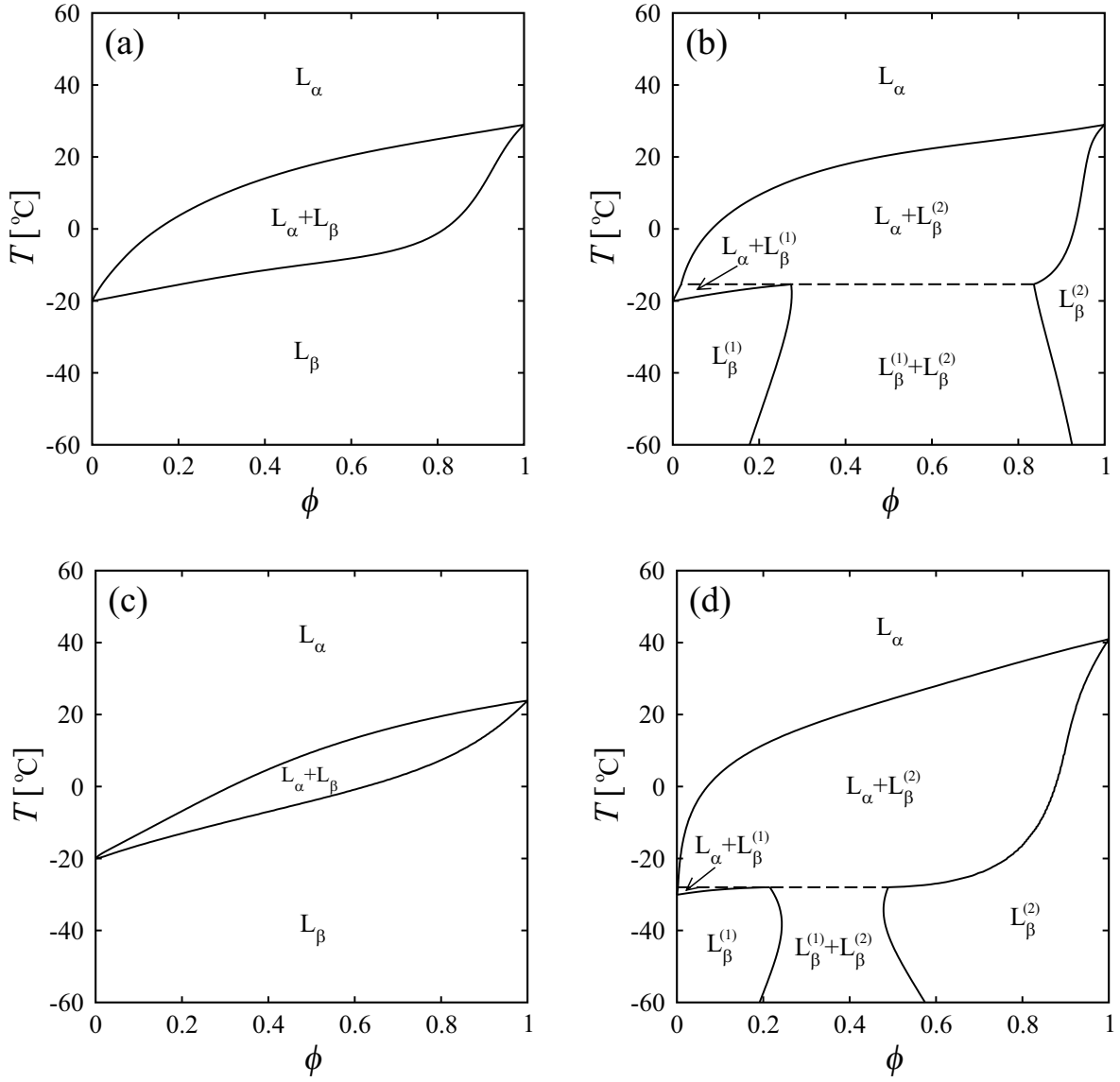

FIG. 6: Phase diagrams of two-component charged membranes as a function of the molar fraction, ϕ, of saturated lipid (either CS or NS) and temperature T. (a) CS/NU membrane with $J = 1.2 \times 10^{-20}$ J and $n_b = 1$ M; (b) CS/NU membrane with $J = 1.8 \times 10^{-20}$ J and $n_b = 1$ M; (c) CS/NU membrane with $J = 1.2 \times 10^{-20}$ J and $n_b = 10$ mM; and (d) NS/CU membrane with $J = 1.2 \times 10^{-20}$ J and $n_b = 1$ M. The other parameters are listed in Table I and are mentioned in the text. The horizontal dashed lines located at $T = -15.3\,^\circ$C in part b and $T = -28.0\,^\circ$C in part d indicate the three-phase coexistence (triple point).

lipid is charged or neutral. Due to the lipid volume conservation, the main-transition temperature of the charged lipid (either CS or CU) is reduced as compared with that of the neutral counterpart. These findings will be further discussed in Sec. IV.

D. Molecular Area in Charged Membranes

In Fig. 8, we show the temperature dependence of the molecular area, Σ, which is calculated from the optimal order parameter, m^*, and Eq. (16). For the CS/NU mixture, the molar fraction ϕ of the CS lipid is varied, and the salt concentration is either $n_b = 1$ M (high salt) or 10 mM (low salt), as shown in Fig. 8 (a) and (b), respectively. In Fig. 8(c), we show the molecular area of the NS/CU mixture for $n_b = 1$ M. Since Σ is independent of the interaction parameter J, the calculation in Fig. 8(a) has been used in generating Fig. 6(a) and (b). Similarly, the calculated Σ values shown in Fig. 8(b) and (c) were used to obtain Fig. 6(c) and (d), respectively. In order to see the change of the molecular area clearly, we ignore here the multiphase coexistence and look at only the minimum of the total free energy, f_{tot}.

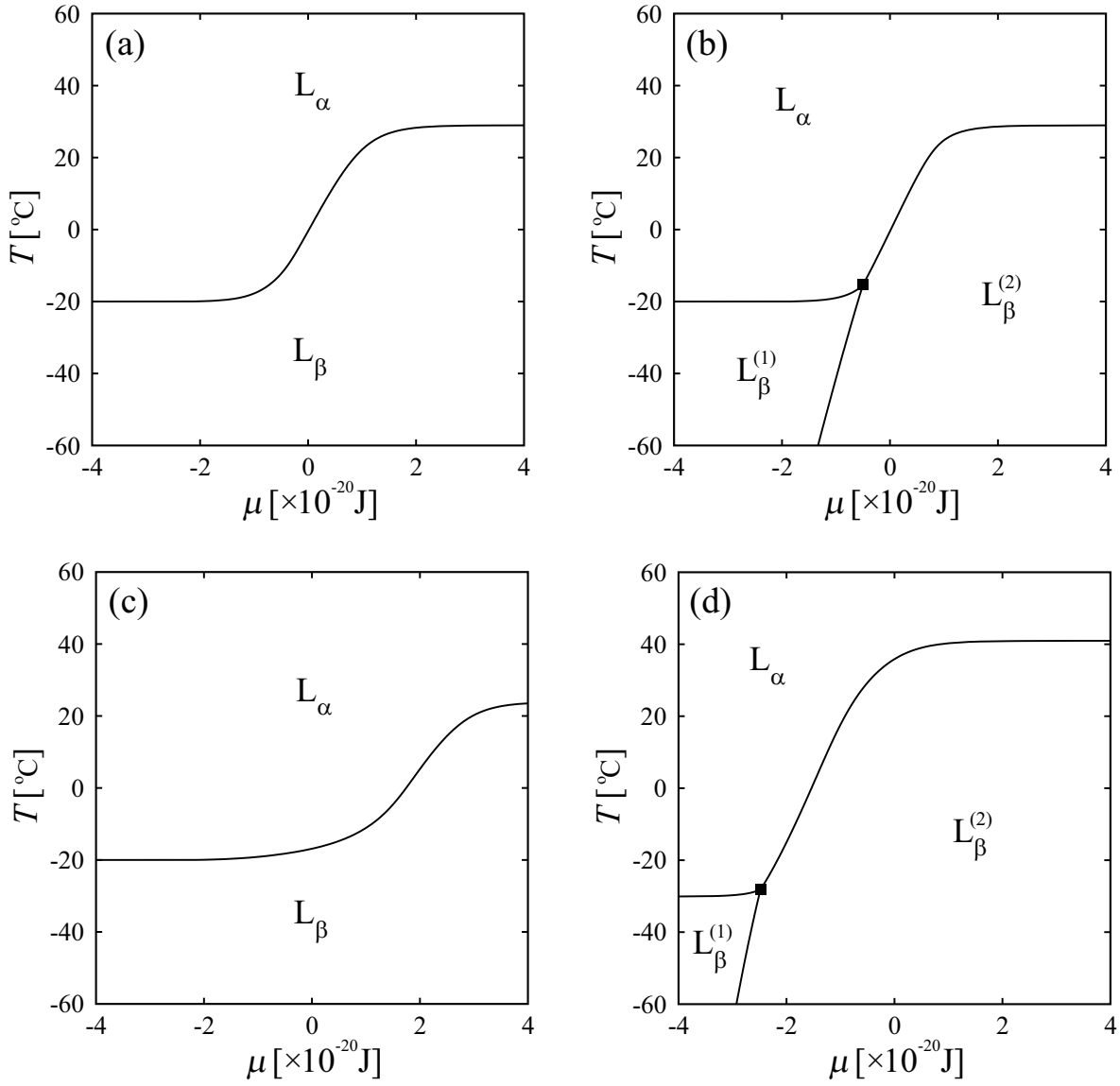

FIG. 7: Phase diagrams of two-component charged membranes as a function of the chemical potential, μ, of saturated lipid (either CS or NS) and temperature T. (a) CS/NU membrane with $J = 1.2\times10^{-20}$ J and $n_{\rm b} = 1$ M; (b) CS/NU membrane with $J = 1.8\times10^{-20}$ J and $n_{\rm b} = 1$ M; (c) CS/NU membrane with $J = 1.2\times10^{-20}$ J and $n_{\rm b} = 10$ mM; and (d) NS/CU membrane with $J = 1.2\times10^{-20}$ J and $n_{\rm b} = 1$ M. The other parameters are listed in Table I and are mentioned in the text. The filled squares located at (μ, T)=$(-0.50\times10^{-20}$ J, $-15.3\,^\circ$C) in part b and $(-2.48\times10^{-20}$ J, $-28.0\,^\circ$C) in part d indicate the triple points.

In Fig. 8(a) and (b), for a pure NU membrane ($\phi = 0$), Σ gradually increases when the temperature is increased approaching the main-transition temperature. As mentioned in Sec. II, the molecular area discontinuously jumps to a larger value as appropriate for the L_α phase at $T_{\rm U}^{**} = -20\,^\circ$C because the main-transition is first-order. In the L_α phase of the NU membrane, Σ takes a constant value, $\Sigma_0 = 65\,$Å^2, because the order parameter m^* always vanishes there.

In the presence of the CS lipid ($\phi > 0$), Σ also increases and exhibits a discontinuous jump at the main-transition temperature. At the transition temperature, as compared with the neutral membranes, Σ for the charged membranes is slightly smaller for the L_β phase but larger for the L_α phase. This tendency can be clearly seen for higher molar fractions of CS lipid ($\phi \approx 1$) or for lower salt concentrations (Fig. 8(b)). As the temperature is further increased from the main-transition temperature, T^{**}, Σ in the L_α phase asymptotically approaches the constant value, $\Sigma_0 = 65\,$Å^2.

The temperature dependence of Σ for the NS/CU mixture is shown in Fig. 8(c). The molecular area first in-

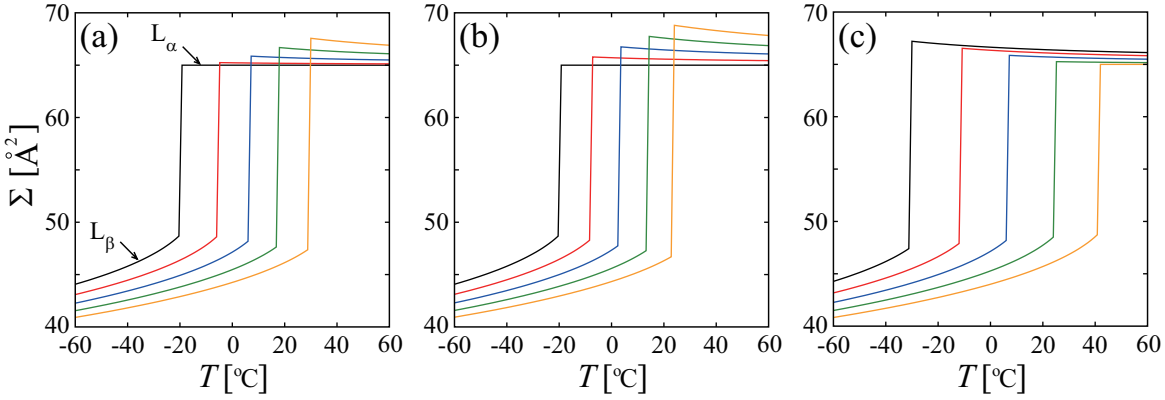

FIG. 8: Plots of molecular area Σ as a function of the temperature T. (a) CS/NU lipid membrane with $n_{\rm b} = 1\,{\rm M}$, (b) CS/NU lipid membrane with $n_{\rm b} = 10\,{\rm mM}$, and (c) NS/CU lipid membrane with $n_{\rm b} = 1\,{\rm M}$. Black, red, blue, green, and orange lines correspond, respectively, to $\phi = 0$, 0.25, 0.5, 0.75, and 1.

creases in the L_β phase and then jumps discontinuously at the main-transition temperature. This molecular area expansion is larger for higher molar fraction of the CU lipid ($\phi \approx 0$). In the next section, we shall discuss in more detail the effect of the lipid volume conservation on the molecular area.

IV. DISCUSSION

Several points merit further discussion. First, we discuss the effect of the interaction parameter J on the phase behavior. As shown in Figs. 4 and 6 for neutral and charged membranes, respectively, the phase-separated region becomes larger as J increases. In particular, we find different coexistence regions such as liquid-liquid ($L_\alpha^{(1)}$+$L_\alpha^{(2)}$) in Fig. 4(b), and solid-solid ($L_\beta^{(1)}$+$L_\beta^{(2)}$) in Fig. 6(b). These coexistence regions do not appear for smaller J value as in Fig. 4(a) and Fig. 6(a). Such a dependence on J was also reported in previous theoretical works [19, 20].

As seen in Fig. 6, the main-transition temperature, T^{**}, is reduced for a single-component charged lipid membrane. The transition temperature of NS lipid is $T_{\rm S}^{**} = 41\,^\circ{\rm C}$, while it is decreased to $T_{\rm S}^{**} \simeq 29\,^\circ{\rm C}$ for CS lipid as in Fig. 6(a) and (b), or to $T_{\rm S}^{**} \simeq 23\,^\circ{\rm C}$ as in Fig. 6(c). The electrostatic repulsion between the charged lipid molecules tends to expand the molecular area, resulting in a decrease of the membrane thickness, while keeping the molecular volume $v = \Sigma\delta$ constant (see Fig. 3). Hence, the molecular volume conservation enhances the phase transition toward the L_α phase, and the main-transition temperature is decreased [39]. For a single-component unsaturated lipid, the reduction of the transition temperature from $T_{\rm U}^{**} = -20\,^\circ{\rm C}$ (for NU) to $-30\,^\circ{\rm C}$ (for CU) can also be explained by the volume conservation constraint (see Fig. 6(d)).

Next, we comment on the effect of the electrostatic interaction on the extension of the phase-separated regions. We have presented the phase behavior of a neutral NS/NU membrane (Fig. 4(a)), a charged CS/NU membrane with a high salt concentration (Fig. 6(a)), and a charged CS/NU membrane with a low salt concentration (Fig. 6(c)). The phase separation takes place below $T = 41\,^\circ{\rm C}$ in Fig. 4(a), between $T = 29\,^\circ{\rm C}$ and $-20\,^\circ{\rm C}$ in Fig. 6(a), and between $T = 23\,^\circ{\rm C}$ and $-20\,^\circ{\rm C}$ in Fig. 6(c). As the electrostatic interaction strength is increased in the order of Figs. 4(a), 6(a) and 6(c), the phase-separated region becomes narrower. For the NS/CU membrane in Fig. 6(d), the phase coexistence occurs below $T = 41\,^\circ{\rm C}$. Although this temperature range coincides with that of neutral NS/NU membranes as in Fig. 4(a), the phase-coexistence region in charged membranes (Fig. 6(d)) is narrower than that in neutral membranes (Fig. 4(a)). Hence, the phase separation is generally suppressed in charged membranes as compared with neutral ones.

Some experiments [25–29] reported that the two-phase coexistence region for charged membranes (containing mainly CU lipid) is narrower than that for neutral membranes, and the phase separation in these membranes can be enhanced again by adding a salt. Compared with two-component neutral membranes (Fig. 4(a)), the phase-separated region of an NS/CU membrane (Fig. 6(d)) becomes narrower due to the electrostatic interactions. This is indeed consistent with experiments. Previous theoretical models for charged membranes [26, 31, 32] have considered only the contributions from the phase separation and the electrostatic interactions. Although these works also reported the suppression of the phase separation in charged membranes, the main-transition was not taken into account. In the present work, we have included this phase transition in order to fully describe the phase behavior of two-component charged membranes. The advantage of our model is that it describes the different phase behavior, distinguishing CS/NU and NS/CU lipid mixtures.

As mentioned in Sec. I, there are two types of two-component charged membranes: CS/NU and NS/CU lipid mixtures. These two cases are presented in Fig. 6(a) and (d), which manifest that the phase-separated region in the former case is narrower than that in the latter one. This is because the difference in the main-transition temperature between the saturated and unsaturated lipids is larger in the NS/CU case (Fig. 6(d)). We note again that the reduction of the transition temperature for charged lipids is induced by the molecular volume conservation.

In general, the larger the difference in the transition temperatures, the stronger the segregation, and the phase separation is enhanced. Himeno *et al.* [29] reported that the phase behaviors of CS/NU and NS/CU lipid mixtures are quite different. In particular, they obtained the liquidus lines and compared the phase separations in CS/NU and NS/CU mixtures with that in an NS/NU mixture. According to their results, the phase separation is enhanced for a CS/NU mixture, whereas it is suppressed for an NS/CU mixture. Although it is difficult to compare directly this experiment with our theory, our model clearly distinguishes between the two different types of charged membranes, and the trends agree with experiments. In the previous experimental work [29], it was considered that there is a counterion mediated attraction between charged saturated lipids, which overcomes the electrostatic repulsion between the charged head groups. For simplicity, this effect was not considered in the present study. However, it will be of interest to consider such added interactions in future theoretical studies in order to make a direct comparison with the experimental results.

We further comment now on the discontinuous jump of the molecular area at the main-transition temperature. For a pure NS lipid membrane ($\phi = 1$ in Fig. 8(c)), the molecular area jumps from $\Sigma = 48.7$ to $65\,\text{Å}^2$ at $T_{\rm S}^{**} = 41\,^\circ$C. For a pure CS lipid membrane ($\phi = 1$ in Fig. 8(a) or (b)), on the other hand, it varies from $\Sigma = 47.4$ to $67.6\,\text{Å}^2$ at $T_{\rm S}^{**} = 29\,^\circ$C in Fig. 8(a), and from $\Sigma = 46.9$ to $68.8\,\text{Å}^2$ at $T_{\rm S}^{**} = 23\,^\circ$C in Fig. 8(b). This means that the main-transition of a CS lipid occurs when the temperature is lower and the molecular area is smaller, as compared with an NS lipid. This behavior can be explained by the electrostatic repulsion between the charged head groups (see Fig. 3). In general, the main-transition is induced when the attraction between the lipids becomes weaker. For CS lipids, the electrostatic repulsion between the lipids acts in addition to the attraction. Hence, the main-transition occurs at a lower temperature and smaller molecular area. Moreover, the molecular area of a CS lipid in the L_α phase is larger than that of an NS lipid ($\Sigma = 65\,\text{Å}^2$) due to the electrostatic repulsion. The increase in the molecular area at the main-transition is more enhanced when the molar fraction of charged lipid is higher.

For higher temperatures, the molecular expansion in two-component charged membranes is suppressed. In the presence of charged lipid, Σ in the L_α phase asymptotically approaches Σ_0 as the temperature is further increased. We recall here that the total free energy of CS/NU or NS/CU membranes is given by Eq. (18) or (19). Taking into account the temperature dependence of $p = 2\pi\ell_{\rm B}/\Sigma_0\kappa = e/\Sigma_0\sqrt{8n_{\rm b}\varepsilon_{\rm w}k_{\rm B}T}$, we note that the relative contribution of the electrostatic free energy vanishes in the high temperature limit. Namely, $f_{\rm el}/(f_{\rm st} + f_{\rm mix}) \to 0$ as $T \to \infty$. This means that the electrostatic interaction becomes irrelevant with respect to the non electrostatic free energies in the high temperature limit, and $\Sigma \to \Sigma_0$.

In neutral membranes, the optimal order parameter m^* vanishes in the L_α phase. On the other hand, in charged membranes, m^* in the L_α phase becomes negative due to molecular volume conservation. Since the order parameter represents the membrane thickness, negative m means an expansion of the molecular area, as shown in Fig. 3. In order to understand why m^* becomes negative, we expand the electrostatic free energy $f_{\rm el}$ of Eq. (17) in powers of m

$$\frac{f_{\rm el}(m,\phi)}{k_{\rm B}T} \approx 2\phi\left[\frac{1-\sqrt{1+(p\phi)^2}}{p\phi} + \ln\left(p\phi+\sqrt{1+(p\phi)^2}\right)\right] - \frac{2\left(1-\sqrt{1+(p\phi)^2}\right)}{p}m - \frac{\left(1-\sqrt{1+(p\phi)^2}\right)^2}{p\sqrt{1+(p\phi)^2}}m^2. \tag{24}$$

The order parameter m is determined by minimizing the total free energy, Eq. (18), which includes Eq. (24). The latter equation is minimized for nonzero m due to the linear term in m because $\sqrt{1+(p\phi)^2} > 1$. Since the stretching free energy $f_{\rm st}$ in Eq. (2) does not include any linear term in m, the total free energy is minimized for a negative $m^* < 0$. As mentioned above, the electrostatic interaction becomes negligible at higher temperatures. Therefore, m^* asymptotically vanishes when the temperature is increased.

In this study, we have used the Poisson-Boltzmann theory to obtain the electrostatic potential for symmetric monovalent salt. Such a mean-field treatment would break down when ion-ion correlations become significant. For example, when multivalent ions are present or a crowding state of charged lipids occurs, it would be important to include ion-ion correlations beyond the mean-field theory. This point will be addressed in a future study. Furthermore, modulated phases in neutral lipid membranes were discussed theoretically by taking into account both the lipid main transition and the spatial dependence of the lipid composition [22]. In the case of a charged lipid membrane, the formation of modulated phases was predicted within the Debye-Hückel approximation without considering the lipid main transition [**?**]. However, the occurrence of such a microphase separation has not yet been reported experimentally for charged bilayer membranes using optical microscopes [25–30]. This is because the characteristic wavelength of the mi-

crophase separation is considered to be of the order of nanometers [40]. Further theoretical and experimental studies are needed in order to investigate the possibility of such microphase separations in charged lipid membranes.

V. CONCLUSIONS

In this work, we have considered phase transitions and separations in binary mixtures of charged membranes. Taking into account the chain main-transition, we have calculated the phase diagrams of two-component charged and neutral lipids. In particular, we have considered a coupling effect between the order parameter and the lipid composition through the molecular volume conservation. We showed that the phase separation in charged membranes is suppressed as compared with the neutral case. Furthermore, as the salt concentration is increased because of screening, the phase separation in charged membranes is enhanced again, signaling the importance of electrostatic interaction.

We have focused on the combination of the lipid hydrocarbon saturation and the charge on the headgroup (either CS/NU or NS/CU). The phase behavior of these two types of binary mixtures of charged/neutral lipids is very different, and is in agreement with recent experiments [26, 28, 29]. We also find that the molecular area of charged/neutral mixtures is smaller in the L_β phase and larger in the L_α, as compared with neutral mixtures. In other words, the discontinuous jump of the molecular area for charged/neutral mixtures is larger than that for the neutral ones. This tendency is clearly seen when the charged lipid fraction is large and/or the salt concentration is low, and can be understood by the electrostatic repulsion between the charged head groups. In general, the phase behavior is significantly influenced by the presence of the charged lipid.

Our model describes the phase behavior of binary mixtures of charged/neutral lipids. In most of the recent experimental studies [25–29], however, the phase separation has been observed in ternary charged lipid mixtures containing cholesterol. Since these studies are motivated by the formation of raft domains enriched in cholesterol, lipid mixtures containing cholesterol are also important from the biological point of view. Putzel and Schick proposed a model [41] for the phase separation in neutral membranes consisting of saturated lipids, unsaturated lipids, and cholesterol. In the future, it will be of interest to consider a model for ternary charged lipid membranes, which will take into account explicitly the specific role of cholesterol, in addition to the effect of charges in lipid mixtures.

Acknowledgments

We thank R. Okamoto for useful discussions. N.S. acknowledges support from the Grant-in-Aid for Young Scientist (B) (Grant No. 26800222) from the Japan Society for the Promotion of Science (JSPS) and the Grant-in-Aid for Scientific Research on Innovative Areas "*Molecular Robotics*" (Grant No. 15H00806) from the Ministry of Education, Culture, Sports, Science, and Technology of Japan (MEXT). T.H. acknowledges support from the MEXT KAKENHI Grant No. 15H00807 and 26103516, JSPS KAKENHI Grant No. 15K12538, and AMED-CREST, AMED. S.K. acknowledges support from the Grant-in-Aid for Scientific Research on Innovative Areas "*Fluctuation and Structure*" (Grant No. 25103010) from MEXT, the Grant-in-Aid for Scientific Research (C) (Grant No. 15K05250) from JSPS, and the JSPS Core-to-Core Program "*International Research Network for Non-equilibrium Dynamics of Soft Matter*". D.A. acknowledges support from the Israel Science Foundation under Grant No. 438/12, the United States-Israel Binational Science Foundation under Grant No. 2012/060, and the ISF-NSFC joint research program under Grant No. 885/15.

[1] K. Simons and E. Ikonen, Nature **387**, 569 (1997).
[2] K. Simons and J. L. Sampaio, Cold Spring Harbor Perspect. Biol. **3**, a004697 (2011).
[3] S. Komura and D. Andelman, Adv. Coll. Int. Sci. **208**, 34 (2014).
[4] S. L. Veatch and S. L. Keller, Phys. Rev. Lett. **89**, 268101 (2002).
[5] S. L. Veatch and S. L. Keller, Biophys. J. **85**, 3074 (2003).
[6] T. Baumgart, S. T. Hess, and W. W. Webb, Nature **425**, 821 (2003).
[7] F. A. Heberle and G. W. Feigenson, Cold Spring Harbor Perspect. Biol. **3**, a004630 (2011).
[8] T. Hamada, R. Sugimoto, T. Nagasaki, and M. Takagi, Soft Matter **7**, 220 (2011).
[9] T. Hamada, Y. Kishimoto, T. Nagasaki, and M. Takagi, Soft Matter **7**, 9061 (2011).
[10] N. Shimokawa, M. Nagata, and M. Takagi, Phys. Chem. Chem. Phys. **17**, 20882 (2015).
[11] L. A. Bagatolli and E. Gratton, Biophys. J. **78**, 290 (2000).
[12] P. A. Beales, V. D. Gordon, Z. Zhao, S. U. Egelhaaf, and W. C. K. Poon, J. Phys.: Condens. Matter **17**, S3341 (2005).
[13] D. Chen and M. M. Santore, Proc. Natl. Acad. Sci. USA **111**, 179 (2014).
[14] D. Chen and M. M. Santore, Langmuir **30**, 9484 (2014).
[15] S. H. Wu and H. M. McConnell, Biochemistry **14**, 847 (1975).
[16] E. J. Luna and M. McConnell, Biochim. Biophys. Acta **470**, 303 (1977).
[17] K. Arnold, A. Lösche, and K. Gawrisch, Biochim. Biophys. Acta **645**, 143 (1981).
[18] A. Blume, R. J. Wittebort, S. K. Das Gupta, and R. G. Griffin, Biochemistry **21**, 6243 (1982).

[19] S. Komura, H. Shirotori, P. D. Olmsted, D. Andelman, Europhys. Lett. **67**, 321 (2004).
[20] S. Komura, H. Shirotori, P. D. Olmsted, J. Phys.: Condens. Matter **17**, S2951 (2005).
[21] R. Elliott, I. Szleifer, and M. Schick, Phys. Rev. Lett. **96**, 098101 (2006).
[22] N. Shimokawa, S. Komura, and D. Andelman, Eur. Phys. J. E **26**, 197 (2008).
[23] T. Yamamoto, R. Brewster, and S. A. Safran, Eur. Phys. Lett. **91**, 28002 (2010).
[24] B. Alberts, A. Johnson, P. Walter, J. Lewis, and M. Raff, *Molecular Biology of the Cell* (Garland Science, New York, 2008).
[25] C. C. Vequi-Suplicy, K. A. Riske, R. L. Knorr, and R. Dimova, Biochim. Biophys. Acta **1798**, 1338 (2010).
[26] N. Shimokawa, M. Hishida, H. Seto, and K. Yoshikawa, Chem. Phys. Lett. **496**, 59 (2010).
[27] M. C. Blosser, J. B. Starr, C. W. Turtle, J. Ashcraft, and S. L. Keller, Biophys. J. **104**, 2629 (2013).
[28] S. Pataraia, Y. Liu, R. Lipowsky, and R. Dimova, Biochim. Biophys. Acta **1838**, 2036 (2014).
[29] H. Himeno, N. Shimokawa, S. Komura, D. Andelman, T. Hamada, and M. Takagi, Soft Matter **10**, 7959 (2014).
[30] H. Himeno, H. Ito, Y. Higuchi, T. Hamada, N. Shimokawa, and M. Takagi, Phys. Rev. E **92**, 062713 (2015).
[31] S. May, D. Harries, and A. Ben-Shaul, Phys. Rev. Lett. **89**, 268102 (2002).
[32] N. Shimokawa, S. Komura, D. Andelman, Phys. Rev. E **84**, 031919 (2011).
[33] R. E. Goldstein and S. Leibler, Phys. Rev. Lett. **61**, 2213 (1988).
[34] R. E. Goldstein and S. Leibler, Phys. Rev. A **40**, 1025 (1989).
[35] D. Andelman, Electrostatic properties of membranes: the Poisson-Boltzmann theory, in Handbook of Biological Physics: Structure and Dynamics of Membranes, edited by R. Lipowsky, E. Sackmann (vol. 1B, Elsevier, Amsterdam, 1995, pp. 603-642 Chapter 12).
[36] D. Andelman, *Soft Condensed Matter Physics in Molecular and Cell Biology*, edited by W. C. K. Poon and D. Andelman (Taylor & Francis, New York, 2006).
[37] D. F. Evans and H. Wennerström, *The Colloidal Domain : Where Physics, Chemistry, Biology and Technology Meet* (John Wiley, New York, 1999).
[38] E. J. W. Verwey and J. Th. G. Overbeek, *Theory of the Stability of Lyophobic Colloids* (Dover Publication, New York, 1999).
[39] F. Jähnig, Biophys. Chem. **4**, 309 (1976).
[40] R. Okamoto, N. Shimokawa, and S. Komura, Europhys. Lett. **114**, 28002 (2016).
[41] G. G. Putzel and M. Schick, Biophys. J. **95**, 4756 (2008).